tial and express their differentiated phenotypes. Biochem Biophys Res Commun 1999;256:184-191.
15. Kocken, JM, de Heer E, Borel Rinkes IH, Sinaasappel M, Terpstra OT, Bruijn JA. Blocking of $\alpha 1\beta 1$ integrin strongly improves survival of hepatocytes in allogeneic transplantation. Lab Invest 1997;77:19-28.
16. Prall F, Nollau P, Neumaier M, Haubeck HD, Drzeniek Z, Helmchen U, et al. CD66a (BGP), an adhesion molecule of the carcinoembryonic antigen family, is expressed in epithelium, endothelium, and myeloid cells in a wide range of normal human tissues. J Histochem Cytochem 1996;44:35-41.
17. Kon J, Ooe H, Oshima H, Kikkawa Y, Mitaka T. Expression of CD44 in rat hepatic progenitor cells. J Hepatol 2006;45:90-98.
18. Yovchev MI, Grozdanov PN, Joseph B, Gupta S, Dabeva MD. Novel hepatic progenitor cell surface markers in the adult rat liver. HEPATOLOGY 2007;45:139-149.
19. Rippin SJ, Hagenbuch B, Meier PJ, Stieger B. Cholestatic expression pattern of sinusoidal and canalicular organic anion transport systems in primary cultured rat hepatocytes. HEPATOLOGY 2001;33:776-782.
20. Sandgren EP, Palmiter RD, Heckel JL, Daugherty CC, Brinster RL, Degen JL. Complete hepatic regeneration after somatic deletion of an albumin-plasminogen activator transgene. Cell 1991;66:245-256.
21. Oinonen T, Lindros KO. Hormonal regulation of the zonated expression of cytochrome P-450 3A in rat liver. Biochem J 1995;309:55-61.
22. Sonnier M, Cresteil T. Delayed ontogenesis of CYP1A2 in the human liver. Eur J Biochem 1998;251:893-898.
23. Sell S. Is there a liver stem cell? Cancer Res 1990;50:3811-3815.
24. Thorgeirsson SS. Hepatic stem cells. Am J Pathol 1993;142:1331-1333.
25. Shafritz DA, Oertel M, Menthena A, Nierhoff D, Dabeva MD. Liver stem cells and prospects for liver reconstitution by transplanted cells. HEPATOLOGY 2006;43(Suppl):89S-98S.
26. Masson NM, Currie IS, Terrace JD, Garden OJ, Parks RW, Ross JA. Hepatic progenitor cells in human fetal liver express the oval cell marker Thy-1. Am J Physiol Gastrointest Liver Physiol 2006;291:G45-G54.
27. Petersen BE, Goff JP, Greenberger JS, Michalopoulos GK. Hepatic oval cells express the hematopoietic stem cell marker Thy-1 in the rat. HEPATOLOGY 1998;27:433-445.
28. Gordon GJ, Coleman WB, Grisham JW. Temporal analysis of hepatocyte differentiation by small hepatocyte-like progenitor cells during liver regeneration in retrorsine-exposed rats. Am J Pathol 2000;157:771-786.
29. Strick-Marchand H, Morosan S, Charneau P, Kremsdorf D, Weiss MC. Bipotential mouse embryonic liver stem cell lines contribute to liver regeneration and differentiate as bile ducts and hepatocytes. Proc Natl Acad Sci U S A 2004;101:8360-8365.
30. Katayama S, Tateno C, Asahara T, Yoshizato K. Size-dependent *in vivo* growth potential of adult rat hepatocytes. Am J Pathol 2001;158:97-105.
31. Mitaka T, Mikami M, Sattler GL, Pitot HC, Mochizuki Y. Small cell colonies appear in the primary culture of adult rat hepatocytes in the presence of nicotinamide and epidermal growth factor. HEPATOLOGY 1992;16:440-447.
32. Asahina K, Shiokawa M, Ueki T, Yamasaki C, Aratani A, Tateno C, et al. Multiplicative mononuclear small hepatocytes in adult rat liver: their isolation as a homogeneous population and localization to periportal zone. Biochem Biophys Res Commun 2006;342:1160-1167.
33. Yoshizato K. Growth potential of adult hepatocytes in mammals: highly replicative small hepatocytes with liver progenitor-like traits. Dev Growth Differ 2007;49:171-184.
34. Gordon GJ, Butz GM, Grisham JW, Coleman WB. Isolation, short-term culture, and transplantation of small hepatocyte-like progenitor cells from retrorsine-exposed rats. Transplantation 2002;73:1236-1243.
35. Brown JJ, Parashar B, Moshage H, Tanaka KE, Engelhardt D, Rabbani E, et al. A long-term hepatitis B viremia model generated by transplanting nontumorigenic immortalized human hepatocytes in Rag-2-deficient mice. HEPATOLOGY 2000;31:173-181.
36. Malhi H, Irani AN, Gagandeep S, Gupta S. Isolation of human progenitor liver epithelial cells with extensive replication capacity and differentiation into mature hepatocytes. J Cell Sci 2002;115:2679-2688.
37. Nowak G, Ericzon BG, Nava S, Jaksch M, Westgren M, Sumitran-Holgersson S. Identification of expandable human hepatic progenitors which differentiate into mature hepatic cells *in vivo*. Gut 2005;54:972-979.

Xenotransplantation 2008: 15: 235–245
Printed in Singapore. All rights reserved
doi: 10.1111/j.1399-3089.2008.00483.x

XENOTRANSPLANTATION

Engraftment of human hepatocytes in the livers of rats bearing bone marrow reconstructed with immunodeficient mouse bone marrow cells

Igarashi Y, Tateno C, Tanaka Y, Tachibana A, Utoh R, Kataoka M, Ohdan H, Asahara T, Yoshizato K. Engraftment of human hepatocytes in the livers of rats bearing bone marrow reconstructed with immunodeficient mouse bone marrow cells.
Xenotransplantation 2008; 15: 235–245. © 2008 Wiley Periodicals, Inc.

Abstract: Background: Previously, we created, a chimeric mouse (humanized mouse), a severe combined immunodeficiency (SCID) mouse whose liver was >90% repopulated with human (*h*)-hepatocytes, which are useful for the testing of drug metabolism and toxicity, as well as a hepatitis B virus and hepatitis C virus-susceptible animal model. However, their small body size and small total blood volume limited the utilization for analytical purposes, which led us to develop a method to create a chimeric rat bearing *h*-hepatocyte-repopulated liver.
Methods: F344 nude rats devoid of T cells were irradiated with X-rays and injected with bone marrow cells (BMCs) from SCID mice (m_{SCID}). The rate of replacement with m_{SCID}-BMCs was evaluated by two-color flow cytometry analysis of peripheral blood mononuclear cells (PBMCs). After m_{SCID}-BMCs repopulated the host bone marrow (BM), the rats were treated with retrorsine, partially hepatectomized (PHx), and transplanted with 5×10^6 *h*-hepatocytes isolated from the chimeric mice. *h*-Albumin (*h*-Alb) concentrations in the host blood and the expression levels of protein and mRNA of hepatocyte differentiation markers in the *h*-hepatocytes were evaluated by ELISA, immunostaining, and reverse transcription-PCR, respectively.
Results: The m_{SCID}-BMCs successfully repopulated the rats, the percentage of mouse cells reaching 94% among host ($r_{nudeF344}$) PBMCs at 4 weeks after *m*-BMC transplantation. *h*-Hepatocytes isolated from the chimeric mice were transplanted to the liver of the m_{SCID}-BMC-repopulated rats. The engrafted *h*-hepatocytes expressed *h*-Alb and *h*-cytochrome P450 (CYP) subtypes and survived showing normal phenotypes until at least 3 weeks post-*h*-hepatocytes transplantation (*h*-HPCT). However, the blood concentrations of *h*-Alb declined at 4 weeks post-HPCT, concomitant with the emergence of both $r_{nudeF344}$- and m_{SCID}-macrophages, suggesting the rejection of *h*-hepatocytes due to the activation of macrophages.
Conclusion: We developed a novel method to create a rat that bears the liver engrafted with *h*-hepatocytes, utilizing a rat with the BM composed of m_{SCID}-BMCs as a host. This *h*-hepatocyte-bearing rat will be a valuable model for studying the immunologic mechanisms involved in xenogeneic transplantation and for generating rats with higher rates of repopulation with *h*-hepatocytes.

Yuka Igarashi,[1,2] Chise Tateno,[2,*] Yuka Tanaka,[1] Asato Tachibana,[2,3] Rie Utoh,[2,†] Miho Kataoka,[2] Hideki Ohdan,[1] Toshimasa Asahara[1] and Katsutoshi Yoshizato[2,4,*]

[1]Department of Surgery, Division of Frontier Medical Science, Program for Biomedical Research, and Hiroshima University 21st Century COE Program for Advanced Radiation Casualty Medicine, Graduate School of Biomedical Sciences, Hiroshima University, [2]Yoshizato Project, CLUSTER, Hiroshima Prefectural Institute of Industrial Science and Technology, Higashi-Hiroshima, Japan, [3]PhoenixBio Co., Ltd, Hiroshima, Japan, [4]Developmental Biology Laboratory and Hiroshima University 21st Century COE Program for Advanced Radiation Casualty Medicine, Department of Biological Science, Graduate School of Science, Hiroshima University, Higashi-Hiroshima, Japan

*Present address: PhoenixBio. Co. Ltd., 3-4-1 Kagamiyama, Higashihiroshima, Hiroshima 739-0046, Japan.
Tel: +81-82-831-0016; Fax: +81-82-831-0017

†Present address: Tokyo Women's Medical University, Institute of Advanced Biomedical Engineering and Science, Kawada-cho 8-1, Shinjuku-ku, Tokyo 162-8666, Japan. Tel: +81-3-3353-8111 (Ext. 30233); Fax: +81-3-3359-6046

Key words: bone marrow transplantation – flow cytometry – hepatocyte transplantation – humanized mice – SCID mice

Abbreviations: BMCs, bone marrow cells; m_{SCID}, SCID mouse; PBMCs, peripheral blood mononuclear cells; BMCT, bone marrow cell transplantation; *h*-Alb, human albumin; $r_{nudeF344}$, F344 nude rats; PHx, partial hepatectomy; HPCT, hepatocytes transplantation; BM, bone marrow; CYP, cytochrome P450; mAb, monoclonal antibody.

Address reprints request to Katsutoshi Yoshizato, Ph.D., PhoenixBio. Co. Ltd., 3-4-1 Kagamiyama, Higashihiroshima, Hiroshima 739-0046, Japan (E-mail: katsutoshi.yoshizato@phoenixbio.co.jp)

Received 5 May 2008;
Accepted 29 May 2008

Introduction

Hepatocytes play prime roles in metabolizing nutrients and detoxifying chemicals in the liver. Rodents, mostly rats, are used for efficacy and safety testing of new medicines. However, the patterns of drug metabolism and detoxification of rodent hepatocytes differ considerably from those of human (*h*) hepatocytes [1,2]. Therefore, *h*-hepatocytes are important for these types of studies, and as sources for hepatocyte-incorporated artificial liver devices and transplantation therapy for the treatment of patients with liver failure. However, the sources and availability of *h*-hepatocytes are rather limited.

To overcome the problems associated with *h*-hepatocytes, we created a mouse with a liver that consists of *h*-hepatocytes, using a liver-injured and immunodeficient animal as the host for *h*-hepatocyte transplantation that had been obtained by crossing an albumin (Alb) enhancer/promoter-driven urokinase-type plasminogen activator (uPA)-transgenic mouse with a severe combined immunodeficiency (SCID) mouse, the offspring being called a uPA/SCID mouse [3]. When transplanted into uPA/SCID mice, *h*-hepatocytes are engrafted and progressively repopulate the host liver, thereby generating mice with livers that consist almost completely of *h*-hepatocytes. These humanized mice mimic quite well the functions of *h*-hepatocytes, so they are useful for the testing of drug metabolism and toxicity, as well as a hepatitis B virus (HBV)- and hepatitis C virus (HCV)-susceptible animal model [3–5]. However, the small body size of this mouse limits its utilization in broader research areas, such as biology, physiology, biochemistry, pharmacy, and pharmacology. The major limitations are small total blood volume and difficulties with surgical manipulations, such as sampling of blood and bile. In addition, abundant metabolic data have been accumulated using rats in pharmacological studies.

The above-mentioned limitations led us to create "humanized" rats for studying *h*-hepatocytes *in vivo*. The advantages of humanized rats over humanized mice are as follows: (1) surgical manipulation is easier; (2) *h*-hepatocyte propagation is expected to be more than 10-fold higher; and (3) data obtained from chimeric rats can be compared with previously accumulated rat metabolic data.

In the present study, we investigated a method to generate "severe" immunodeficiency in nude rats that lack T cells. SCID mouse (m_{SCID})-bone marrow cells (BMCs) were introduced into the lethally irradiated nude rats. These rats ("SCID-rats") were subjected to retrorsine treatment and partial hepatectomy (PHx), followed by *h*-hepatocyte transplantation (*h*-HPCT). The yielded rats were characterized with respect to the engraftment, proliferation, and functions of the *h*-hepatocytes. As a result, we were able to generate the *h*-hepatocyte-bearing SCID rat whose bone marrow (BM)-related cells had been mostly (>94%) replaced with m_{SCID}-BM-derived cells, although the *h*-hepatocytes did not show a significant degree of replication.

Methods

Animals

Fischer 344 nude rats (F344/N Jcl-*rnu*/*rnu*) aged 4 weeks and SCID mice (Fox Chase SCID C.B-17/lcr-*scid*/*scid*Jcl) aged 6 weeks were purchased from CLEA Japan (Osaka, Japan). All animals were maintained under pathogen-free conditions and in compliance with the guidelines of Hiroshima University and the Hiroshima Prefectural Institute of Industrial Science and Technology.

Conditioning of F344 nude rats

Host BMCs were abrogated by whole-body X-ray irradiation of F344 nude rats [6]. The animals were exposed twice to X-rays. The first irradiation dose was fixed at 10 Gy [6]. Three days later, the rats received the second irradiation at different doses (4, 6, 8, and 10 Gy) for dosage optimization. These irradiation regimens are indicated in a simple way herein. For example, the regimen in which the second irradiation was 4 Gy is indicated as "10 + 4."

Transplantation of m_{SCID}-BMCs into conditioned rats

The m_{SCID}-BMCs were flushed out from the femurs and tibias of SCID male mice with Medium 199 (Sigma–Aldrich, Tokyo, Japan) containing 4 μg/ml gentamycin (Sigma–Aldrich) and 0.01 M Hepes buffer (Gibco, Invitrogen, Tokyo, Japan) using a 26G needle (TERUMO, Tokyo, Japan). The m_{SCID}-BMCs were mechanically resuspended in the medium by gentle aspiration through a 5-ml pipette, passed through a 40-μm-mesh nylon filter (BD Falcon, Tokyo, Japan), pelleted at 600 *g* for 5 min, and resuspended. Viable cells were counted under a microscope using the trypan blue exclusion test. The irradiated rats were transplanted with 10^8 m_{SCID}-BMCs in 500 μl of Medium 199 via the tail vein 1 day after the second irradiation. In the present study, the rats with m_{SCID}-BMCs were designated as SCID rats, since the replacement rate of the

peripheral blood mononuclear cells (PBMCs) with m_{SCID}-PBMCs was quite high (94%).

FACS analysis of hematopoietic chimerism

Blood samples (300 µl per rat) were collected using a heparinized syringe once per week after *m*-bone marrow cells transplantation (BMCT). The blood cells were lysed with ammonium chloride–potassium carbonate lysis buffer consisting of 0.15 M NH_4Cl, 10 mM $KHCO_3$, and 0.1 mM EDTA-Na_2 in 500 ml of MilliQ water, washed twice, and the final pellets containing PBMCs were suspended in FACS buffer, phosphate-buffered saline containing 1.0 mg/ml bovine serum Alb fraction V (Roche Diagnostics K.K., Tokyo, Japan) and 1.0 mg/ml sodium azide (Nacalai Tesque K.K., Kyoto, Japan). The PBMCs were resuspended in FACS buffer and divided equally into test tubes. The PBMCs were stained for 30 min at 4 °C with the following immunofluorescently labeled monoclonal antibodies (mAbs; all from BD Pharmingen, Tokyo, Japan) with specificity for the rat (*r*) or mouse (*m*): FITC-labeled *m*-anti-*r* RT1A and *r*-anti-*m*-biotinylated H-$2D^d$ for class I MHC antigens; FITC-labeled *m*-anti-*r*-CD11b/c and phycoerythrin (PE)-labeled *r*-anti-*m*-CD11b for macrophages; FITC-labeled *m*-anti-*r*-CD4 and PE-labeled *r*-anti-*m*-CD4 for CD4-T cells; PE-labeled *m*-anti-*r*-CD8 and FITC-labeled *r*-anti-*m*-CD8 for CD8-T cells; FITC-labeled *m*-anti-*r*-B220 and PE-labeled *r*-anti-*m*-CD19 for B cells; and biotinylated *m*-anti-*r*-CD161a and FITC-labeled *r*-anti-*m*-CD49/Pan for NK cells. The biotinylated mAbs were visualized with PE-labeled streptavidin for 15 min at 4 °C in the dark. Stained cells were analyzed using FACScalibur (Becton Dickinson, Tokyo, Japan). Dead cells were excluded from the analysis by forward-scatter and propidium iodide (PI) staining. The FACS data were analyzed using the Win MDI software.

Isolation of *h*-hepatocytes from humanized mice

Humanized mice were generated as described previously [3]. Briefly, $7.5–10.0 \times 10^5$ cryopreserved *h*-hepatocytes from a 4-year-old boy (BD Gentest) were transplanted into uPA/SCID mice. Liver cells were isolated from the chimeric mice with >10 mg/ml *h*-Alb in their blood using the two-step collagenase perfusion method [7] and centrifuged three times at 50 *g* for 2 min. The pellet was suspended in Dulbecco modified Eagle's medium (Gibco, Invitrogen) that contained 10% fetal bovine serum, and the living cells were counted using the trypan blue exclusion test. The purity of the *h*-hepatocytes in the preparation was >90%, as determined by FACS analysis with *h*-hepatocyte-specific antibody (K8216) that had been prepared as described below. We confirmed that when transplanted into a new uPA/SCID mouse, these *h*-hepatocytes engrafted the liver, proliferated therein, and formed colonies (data not shown).

Preparation of K8216

A BALB/c mouse was immunized with 10^7 subcultured *h*-hepatocytes [8] three times weekly for 3 weeks with a booster injection of 2.5×10^7 subcultured *h*-hepatocytes after the last immunization. Frozen sections of human and murine livers were incubated with hybridoma supernatants obtained by conventional methods at the Institute of Immunology (Tokyo, Japan) and with the secondary antibodies of Alexa 488-labeled anti-*m*IgG goat sera (Molecular Probes, Invitrogen). The hybridoma for which the supernatant reacted with the plasma membranes of *h*-hepatocytes, but not with those of *m*-hepatocytes, was selected. The supernatant was analyzed by FACS for reactivity with the surfaces of hepatocytes. Thus, the *m*- and *h*-hepatocytes were incubated with the hybridoma supernatant and the secondary antibodies, and analyzed in the FACS Vantage (Becton Dickinson) using a 100-µm nozzle. Fluorescence was measured after excitation at 488 nm through a 530-nm filter (FL1) with a 4-decade logarithmic amplification. This analysis showed that the antibodies reacted with the cell surfaces of *h*-hepatocytes, but not with those of *m*-hepatocytes. The hybridoma was injected intraperitoneally (i.p.) into nude mice, and the antibodies in the ascites (designated as K8216) were purified by ammonium sulfate sedimentation.

Transplantation of *h*-hepatocytes into SCID rats

Retrorsine is used as a strong anti-mitogenic agent for rat hepatocytes [9]. *h*-Hepatocytes isolated from the chimeric mice as described above were transplanted in retrorsine- and PHx-treated rats as reported previously [9] with modifications. The m_{SCID}-BMC-bearing rats were given two i.p. injections of retrorsine (30 mg/kg body weight; Sigma–Aldrich) 2 weeks apart, to inhibit hepatocyte proliferation in the host rat liver. Histologic sections of the livers were obtained from the SCID rats 3 weeks after the second injection of retrorsine and stained with hematoxylin and eosin. These sections showed that most of the host hepatocytes had become megakaryocytes (data

not shown), reflecting the inhibition of hepatocyte cell division.

Three weeks after the second injection, the animals were anesthetized by ether inhalation and subjected to 40% PHx. The lateral right lobe was exposed by a midline incision near the xiphisternum and resected, and the incision was closed with a suture. The ileocecum was exposed by a midline incision at the hypogastric region. The *h*-hepatocytes obtained from the chimeric mice were suspended at 2.5×10^6 and 5.0×10^6 cells in 0.5-ml aliquots and transplanted into the SCID rats via the portal vein using a syringe. Murine plasma thrombin (Sigma–Aldrich) was used for hemostasis. Serum samples (50 μl) were collected from the tail vein periodically after *h*-HPCT and used for measuring *h*-Alb concentrations by ELISA (Human Albumin Sensitive ELISA Kit; Cygnus Technologies, Inc., Southport, NC, USA). In preliminary studies, to optimize the number of *h*-hepatocytes for transplantation, we obtained data showing higher rates of the engraftment and the survival of the transplanted cells in the host liver when 5.0×10^6 cells were transplanted compared with the case of transplantation of 2.5×10^6 cells. Therefore, we present herein the results of transplantation experiments with 5.0×10^6 *h*-hepatocytes.

Immunohistochemistry

The rat livers were harvested at 3 and 4 weeks after *h*-HPCT. The rats were all injected i.p. with bromodeoxyuridine (BrdU, Wako Pure Chemical Industries, Ltd., Osaka, Japan) at 10 μl/g body weight 1 h before killing. Cryosections (5-μm thickness) were fixed in cold acetone, blocked with 10% goat or donkey serum for 30 min at room temperature. Sections were incubated with *m*-anti-*h*-cytokeratin 8/18 (*h*CK8/18) mAbs (Cappel Laboratories Inc., West Chester, PA, USA), to distinguish the *h*-hepatocytes. The primary Abs were visualized with Alexa 488-labeled goat anti-*m*-IgG (Molecular Probes). As a measure of the functions of engrafted *h*-hepatocytes, cryosections were incubated with the *m*-anti-*h*-CK8/18 mAbs and rabbit anti-*h*-cytochrome P450 (CYP) 2D6 (Daiichi Pure Chemicals) or 2E1 (Affiniti) mAb (double staining). The primary Abs were visualized with Alexa 488-labeled donkey anti-*m*-IgG (Molecular Probes) or Alexa 594-labeled donkey anti rabbit-IgG. Formalin-fixed paraffin sections (5-μm thickness) were incubated with *m*-anti-*h*-cytokeratin 18 mAb (DakoCytomation) and goat anti-*h*-Alb antibody (Bethyl Laboratories) for double staining, or with goat anti-*h*-Alb antibody and *m*-anti-BrdU mAb (DakoCytomation) for double staining. The primary Abs were visualized with Alexa 488-labeled donkey anti-*m*-IgG or anti goat-IgG or Alexa 594-labeled donkey anti goat-IgG or anti-*m*-IgG (Molecular Probes). The paraffin sections were exposed to microwaves in Target Retrieval Solution (DakoCytomation), to activate the antigens. The *r*- and *m*-macrophages (Kupffer cells) were identified in the SCID rat liver as follows. Cryosections were prepared from the livers of rats at 2 and 7 weeks after m_{SCID}-BMCT, and at 3 and 4 weeks after *h*-HPCT. The sections were incubated with *r*-anti-*m*-macrophage mAb (BM8; BMA Biochemicals, Augst, Switzerland) or *m*-anti-*r*-macrophage mAb (ED2; BMA Biochemicals). The primary Abs were visualized with Alexa 488-labeled goat anti-*m*-IgG and Alexa 594-labeled goat anti-*r*-IgG (Molecular Probes). All sections were counterstained with Hoechst (bisbenzimide; Sigma–Aldrich).

RNA extraction and reverse transcription-PCR

Total RNA samples were extracted with ISOGEN (Nippon Gene, Tokyo, Japan) from the livers of normal F344 nude rats and from rats and mice both bearing *h*-hepatocyte. The RNA samples (1 μg each) were reverse-transcribed at 42 °C for 90 min in a 20-μl reaction mixture that contained random hexamers (Invitrogen) using PowerScript Reverse Transcriptase (Clontech). PCR was performed with rTaq (Takara Bio, Shiga, Japan) under the following conditions: 94 °C for 5 min, followed by 30–40 cycles of denaturing at 94 °C for 30 s, annealing at 54–60 °C for 30 s, and extension at 72 °C for 30 s. The following genes were subjected to semi-quantitative PCR under the conditions listed in Table 1 using primer sets that amplify only human gene (*h*) or mouse, rat, and human gene (*mrh*): *h*-Alb, *h*-α1-antitrypsin (*h*-AAT), *h*-glucose-6-phosphatase (*h*-G6P), *h*-hepatocyte nuclear factor 4 (*h*-HNF-4), cytochrome P450 (*h*-CYP1A2, 3A4, 2E1, 2D6) and *rmh*-glyceraldehyde-3-phosphate dehydrogenase (*mrh*-GAPDH). The amplified PCR products were analyzed by electrophoresis in 2% agarose gels (agarose 36GU; Funakoshi Co., Ltd., Tokyo, Japan) or 4% agarose gels (NuSieve 3:1 agarose; BioWhittaker Molecular Applications) and visualized under UV illumination after ethidium bromide staining.

Results

Generation of SCID rats

F344 nude rats were subjected to X-ray irradiation under the regimen described above and were transplanted 1 day later with 10^8 m_{SCID}-BMCs.

Table 1. Primer sets for RT-PCR

Gene name	Forward primers	Reverse primers	Products size (bp)	Annealing temp. (C°)	Cycles
h-Alb	tgccgaagtggaaaatgatgag	gcaagtctcagcagcagcacg	179	60	40
h-AAT	acccttttgaagtcaaggacaccg	ccattgctgaagaccttagtgatgc	360	60	40
h-G6P	tgggatccagtcaacacattac	caaaacccaccagtatggacgc	234	58	40
h-HNF-4	tcacctcccccgtctcc	Tgcgatgctggcaatctt	61	60	40
h-CYP1A2	agactgcctcctccggg	cagggttaggcaggtagcg	62	60	40
h-CYP3A4	tgtgaggaggtagatttggctc	tcaggaggagttaatggtgctaa	80	60	40
h-CYP2E1	cagcacaactctgagatatgggc	gggcatctcttgcctatcctt	132	60	40
h-CYP2D6	gtccaacaggagatcgacga	ggcatgtgagcctggtca	70	60	40
mrh -GAPDH	accacagtccatgccatcac	tccaccaccctgttgctgta	451	54	30

h, human-specific; *mrh*, mouse-, rat-, and human specific.

Table 2. Survival rates of the hosts after different X-ray dosages in the presence or absence of *m*-BMCT

Second irradiation with X-rays (Gy)	*m*-BMCT	Number of animals: Total	Dead before 7 weeks	Alive until 7 weeks	FACS analysis
0	–[a]	7	0	7	2
4	+	2	0	2	2
4	–	2	0	2	0
6	+	2	0	2	2
6	–	2	0	2	0
8	+	2	0	2	2
8	–	2	0	2	0
10	+	48	0	48	27
10	–	9	9	0	0

[a]Without *m*-BMCT.

The survival rates of the hosts under these regimens are summarized in Table 2. Irrespective of the dosage of the irradiation and the *m*-BMCT, all animals were alive beyond 7 weeks after the start of experiment including the most severe regiment except the animals that were irradiated with "10 + 10," but not received the *m*-BMCT. These rats were in severe anemia and all dead before 7 weeks. They had low body weight at the time of death, the cause of which was most likely BM failure.

We investigated the chimerism of the PBMCs in the host blood by two-color flow cytometry once a week after transplantation of the m_{SCID}-BMCs (Fig. 1). The changes in the occupancy of MHC class I^+ cells, macrophages, and NK cells after *m*-BMCT are shown in Fig. 1(A,B) for *m*- and *r*-cells, respectively. The populations of *m*-MHC class I^+ cells and macrophages increased with time post-transplantation as shown in Fig. 1(A a-1, a-2), respectively. These rates of increase became more pronounced as the second irradiation dosage was increased. The regimen "10 + 10" allowed the m_{SCID}-BMCs to repopulate almost completely the *r*-peripheral blood (94.5% *m*-MHC class I^+ cells) at 5 weeks post-*m*-BMCT (Fig. 1A a-1). Under "10 + 10," the percentages of *m*-macrophages at 1 week post-BMCT were 61.3% and increased to 93.1% at 5 weeks (Fig. 1A a-2). Originally, *m*-NK cells occupied 20–30% of the m_{SCID}-PBMC fraction. But their occupancy in the hosts was < 3% under all the tested regimens (Fig. 1A a-3), indicating that the *m*-NK cells did not proliferate therein after transplantation. As expected, the populations of *r*-MHC class I^+ cells, macrophages, and NK cells decreased with time under all the tested irradiation regimens (Fig. 1B). These rates of decrease became more pronounced as the second irradiation dosage was increased.

Similarly, we determined the changes in the occupancy of *m*- and *r*-$CD8^+$ T cells, $CD4^+$ T cells, and B cells. However, the occupancy of the *m*-cells was all quite low (<0.1%) to extract any significant conclusion. The occupancy of the *r*-cells was 2–15% and showed a tendency to decrease with the increase in the dosage of second irradiation (data not shown). From these results, we concluded that "10 + 10" is optimal for myeloablation. The level of reconstitution with m_{SCID}-BMCs reached as high as 94% under this regimen.

h-Hepatocyte-transplantation into retrorsine- and PHx-treated SCID-rats

h-Hepatocytes were isolated from chimeric mice with replacement index (RI) > 85% and, 5.0×10^6 cells each, were injected into 12 retrorsine-treated and 40% PHx SCID rats (#1–12). Rats that did not receive m_{SCID}-BMCs were similarly transplanted with *h*-hepatocytes as control animals. Eight (#1–8) were alive at least until 3 weeks (survival rate, approximately 67%). The average blood *h*-Alb levels of these rats 1 week post-*h*-HPCT were 21.8 ± 10.9 ng/ml (n = 8), which slowly increased to 29.6 ± 10.9 ng/ml (n = 8) three weeks later. Blood *h*-Alb concentrations were individually monitored for these eight animals during the experimental period as a measure of growth of *h*-hepatocyte colonies (Fig. 2). One rat (#7) died 3 weeks post-transplantation, and the remaining

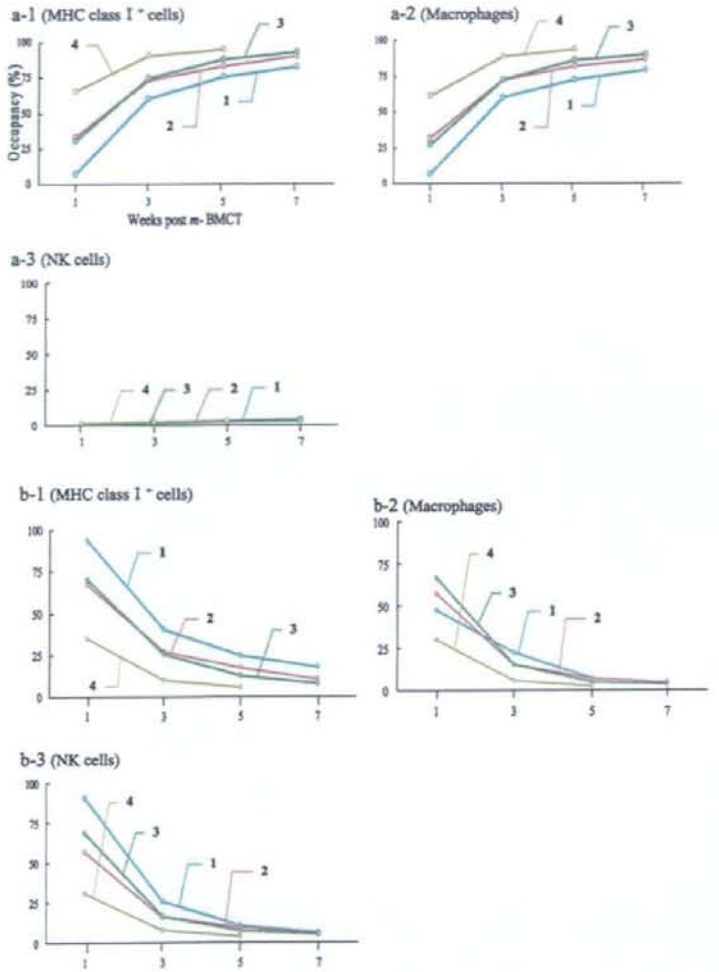

Fig. 1. Replacement of *r*-PBMCs with *m*-PBMCs by transplanting m_{SCID}-BMCs into SCID rats. F344 nude rats were subjected to four different X-ray irradiation (Gy) regimens ("10 + 4," "10 + 6," "10 + 8," "10 + 10") and transplanted with 10^8 m_{SCID}-BMCs 1 day after the second round of irradiation. The lines attached with Arabic numerals, 1, 2, 3, and 4 in the graphs represent individual rats irradiated according to "10 + 4," "10 + 6," "10 + 8," and "10 + 10" regimens, respectively. PBMCs were isolated at 1, 3, and 5 weeks post-*m*-BMCT from the rats and analyzed by two-color flow cytometry. Three types of cells were analyzed as PBMCs: MHC class I^+ cells (a-1 and b-1 for *m*- and *r*-cells, respectively), macrophages (a-2 and b-2 for *m*- and *r*-cells), and NK cells (a-3 and b-3 for *m*- and *r*-cells). *m*- and *r*-MHC class I^+ cells were detected as H-2D- and RT1A-positive ($H\text{-}2D^+$- and $RT1A^+$-) cells, respectively. *m*- and *r*-Macrophages were detected as $CD11b^+$- and $CD11b/c^+$-cells, respectively. *m*- and *r*-NK cells were detected as $CD49/Pan^+$- and *r*-$CD161a^+$-cells, respectively. The occupancy (%) of each type of cells was determined and is plotted against weeks post-*m*-BMCT. (A) Changes in the percentages of *m*-PBMCs. a-1. MHC class I^+-cells. (a-2) Macrophages. (a-3) NK cells. (B). Changes in the percentages of *r*-PBMCs. (b-1) MHC class I^+-cells. (b-2) Macrophages. (b-3) NK cells.

seven rats were kept for an additional 1 week, at which time the blood *h*-Alb levels were determined and the animals were killed. The blood *h*-Alb levels were detectable in all the tested rats at 1 week post-*h*-HPCT, thereafter these levels increased slightly but continuously to 3 weeks in four rats (#1, 2, 3, and 5). However, the levels decreased at 4 weeks post-*h*-HPCT. Animals #4 and #6 showed continuous decreases in *h*-Alb levels through 4 weeks (#4) and 3 weeks (#6) post-*h*-HPCT. Rat #1 showed an exceptionally high *h*-Alb level (95 ng/ml) at 3 weeks post-*h*-HPCT. In contrast, the blood *h*-Alb levels were undetectable during the experimental period in the unconditioned control rats that had received *h*-hepatocytes.

Expression of hepatocyte-specific genes and proteins by *h*-hepatocytes in SCID mice

RNAs were extracted for RT-PCR from the frozen liver tissues of SCID rats that had been transplanted with 5.0×10^6 *h*-hepatocytes shown in Fig. 2. Similarly, RNAs were extracted from normal nude rat livers (negative control) and from the livers of the chimeric mice transplanted with the same donor *h*-hepatocytes (positive control). All the livers of the tested SCID rats contained *h*-hepatocytes that expressed *h*-Alb, *h*-AAT, *h*-G6P, *h*-HNF-4, *h*-CYP1A2, 3A4, 2E1, and 2D6 mRNAs (Fig. 3). Liver sections prepared from the SCID rats used for RT-PCR were subjected to immunostaining for *h*-CK8/18, *h*-Alb, CYP2D6, 2E1, and BrdU

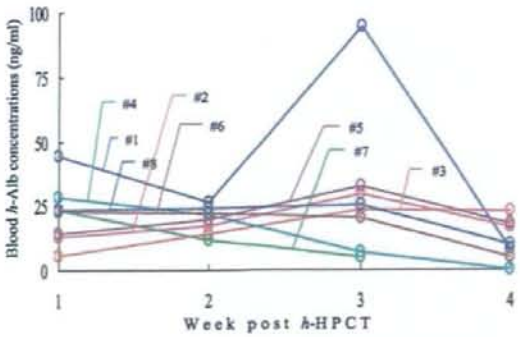

Fig. 2. Blood *h*-Alb concentrations in SCID rats post-*h*-HPCT. *h*-Hepatocytes (5.0×10^6 cells) were transplanted into the livers of retrorsine- and PHx-treated SCID rats. The *h*-Alb levels were determined in the eight rats (#1 through #8) at 1, 2, and 3 weeks. Animal #7 died 3 weeks post-*h*-HPCT. The *h*-Alb levels in the remaining seven rats were determined at 4 weeks post-*h*-HPCT.

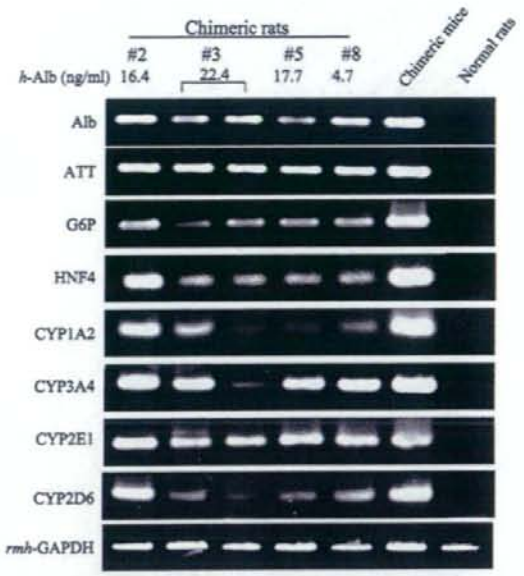

Fig. 3. Expression profiles of *h*-hepatocyte-specific genes in SCID rat livers. Total RNAs were extracted from the livers of normal nude rats and *h*-hepatocyte-chimeric SCID rats, and also from *h*-hepatocyte-chimeric mice from which the *h*-hepatocytes for transplantation into the SCID rats had been isolated. The RNA samples were subjected to PCR to measure the expression levels of the *h*-Alb, *h*-ATT, *h*-G6P, *h*-HNF-4, *h*-CYP1A2, 3A4, 2E1, and 2D6 genes. GAPDH mRNAs were measured as the reference, to ensure equivalent amounts of the tested RNA were used with primers common to the rat, human, and mouse species. Animals #2, 3, 5, and 8 indicated below the "Chimeric rats" tag correspond to the animals #2, 3, 5, and 8 shown in Fig. 2. The blood *h*-Alb concentrations of the tested animals are shown at the tops of the panels.

(Fig. 4). The *h*-CK18$^+$ cells expressed *h*-Alb (Fig. 4a–c). The *h*-CK8/18$^+$ colonies expressed CYP2D6 (Fig. 4d–f) and 2E1 (Fig. 4g–i). BrdU$^+$ cells were observed in *h*-Alb$^+$ cells (Fig. 4j–l). These results suggest that some of the engrafted *h*-hepatocytes are in the S-phase of the cell cycle, and that the engrafted *h*-hepatocytes are able to maintain normal functions in the rat liver tissues. The engrafted *h*-hepatocyte were able to frequently form colonies containing greater than five hepatocytes in all the tested seven animals at 4 weeks post-*h*-HPCT. There were some colonies that contained more than 10 cells in five animals.

Macrophage activation in *h*-hepatocyte-transplanted SCID rat livers

Recently, liver reticuloendothelial macrophages (Kupffer cell) were reported to reject xenogeneic cells through the interspecies incompatible CD47 signaling [10,11]. At 5 weeks post-*m*-BMCT most (~94%) of the macrophages in the PBMCs were derived from the SCID mice (Fig. 1). X-ray irradiated nude rats were transplanted with m_{SCID}-BMCs and liver tissues were removed at early (2 weeks) and late (7 weeks) time-points post-*m*-BMCT. Double-immunostaining was performed to detect and localize *m*- and *r*-macrophages in the liver sections, using the BM8 and ED2 antibodies, respectively (Fig. 5a,b). Both ED2$^+$-*r*-green and BM8$^+$-*m*-red macrophages (Kupffer cells) were scattered throughout the liver at 2 weeks post-*m*-BMCT (Fig. 5a). The ED2$^+$ cells were considered to be dying *r*-macrophages likely due to the X-ray-induced damages because they showed abnormal morphology and weak fluorescence. Although both *r*- and *m*-macrophages were similarly observed throughout the liver at 7 weeks post-*m*-BMCT, ED2$^+$-cells appeared that were morphologically normal and had brighter fluorescence than those at 2 weeks (Fig. 5b). These cells were considered to be *r*-macrophages that escaped X-ray-induced damage and had repopulated the host liver or some X-ray-resistant host progenitor cells had differentiated into macrophages.

Similar double-immunostaining was carried out for the seven *h*-hepatocyte-bearing rats #1–8 as shown in Fig. 2 that had been transplanted with *h*-hepatocyte at 11 weeks post-*m*-BMCT. The liver tissues from these animals at 4 weeks post-*h*-HPCT were used for immunostaining. These seven rats were classified into two groups according to the blood level of *h*Alb. One was the group of three rats (#2, 3, 5) that showed *h*Alb > 15 ng/ml at 4 weeks post-HPCT and the other was that of four rats (#1, 4, 6, 8) with *h*Alb < 10 ng/ml. We

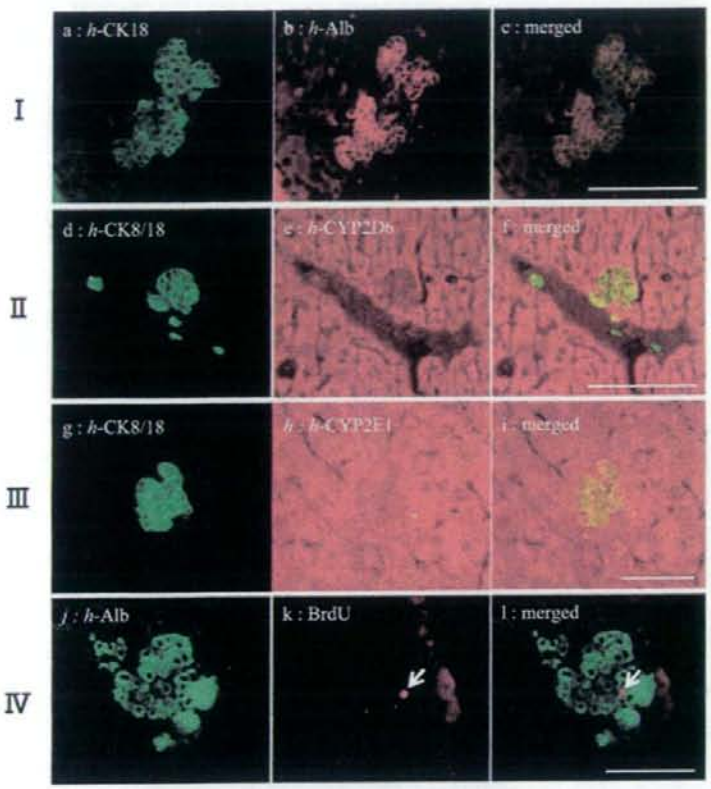

Fig. 4. Characterization of *h*-hepatocytes in the host liver. The rat liver was harvested at 4 weeks post-*h*-HPCT. Some animals were given BrdU 1 h before harvesting. These livers were processed to histological examinations. Four sections (sections I–IV) are presented here. The sections I and IV were formalin-fixed paraffin-processed for *h*-CK18, *h*-Alb, and BrdU staining. The sections II and III were cryo-processed for *h*-CK8/18, *h*-CYP 2D6, and *h*-CYP2E1. The section I was subjected to double immunostaining for *h*-CK18 (a) and *h*-Alb (b). Section II: double immunostaining for *h*-CK8/18 (d) and *h*-CYP 2D6 (e). Section III: double immunostaining for *h*-CK8/18 (g) and *h*-CYP2E1 (h). Section IV: double immunostaining for *h*-Alb (j) and BrdU (k). Images c, f, i, and l are merged photographs of a and b, d and e, g and h, and j and k, respectively. Scale bar = 20 μm.

consistently observed that immunosections of the group with *h*Alb > 15 ng/ml showed the distributions and the size of the *r*- and *m*-macrophages similar to those depicted in Fig. 5b as shown in Fig. 5c in which the liver of rat #5 is presented as a representative example. In contrast, $BM8^{+}$-*m*-macrophages became larger in size in the liver of the group with *h*Alb > 15 ng/ml as shown in Fig. 5d in which an immunosection from rat #6 is presented. We quantified the red colored areas (*m*-macrophage areas) in the photos shown in Fig. 5c,d as a measure of cell size using an image analyzer. The average red area per unit measured area of the rat with with *h*Alb > 15 ng/ml was ~3-fold larger than that with *h*Alb < 10 ng/ml. It is generally accepted that macrophages become enlarged when activated. Therefore, assuming that a *h*Alb concentration < 10 ng/ml predicts that the *h*-hepatocytes will not survive due to rejection by the host, we propose that macrophage activation limits the proliferation and survival of *h*-hepatocytes in SCID rats. The blood *h*-Alb concentration of rat #1 was relatively high (~95 ng/ml) at 3 weeks post-*h*-HPCT, but dropped to < 10 ng/ml at 4 weeks post-*h*-HPCT, most probably due to the rejection of *h*-hepatocytes.

Discussion

We are able to generate reproducibly, and in a stable form, SCID mice with livers that comprise mainly *h*-hepatocytes [3]. Several such immunodeficient and liver-injured mice have been used as hosts for the repopulation of *h*-hepatocytes, including uPA/SCID/beige mice [12], uPA/SCID mice [3,13], recombination activation gene 2 (*Rag-2*) knockout (KO) mice [14], and Fah KO/Rag2KO/IL2RγcKO mice [15].

In the present study, we explored the possibility of creating immunodeficient rats that are suitable for *h*-hepatocyte transplantation. Initially, we irradiated nude rats with X-rays, to eliminate their BMCs, and we then transplanted *m*-BMCs into the rats. Irradiation with the optimal regimen (10 + 10) allowed the m_{SCID}-BMCs to replace almost completely the *r*-PBMCs (the replacement rate of mouse MHC class I cells was 94%) at 5 weeks post-*m*-BMCT. The obtained SCID rats

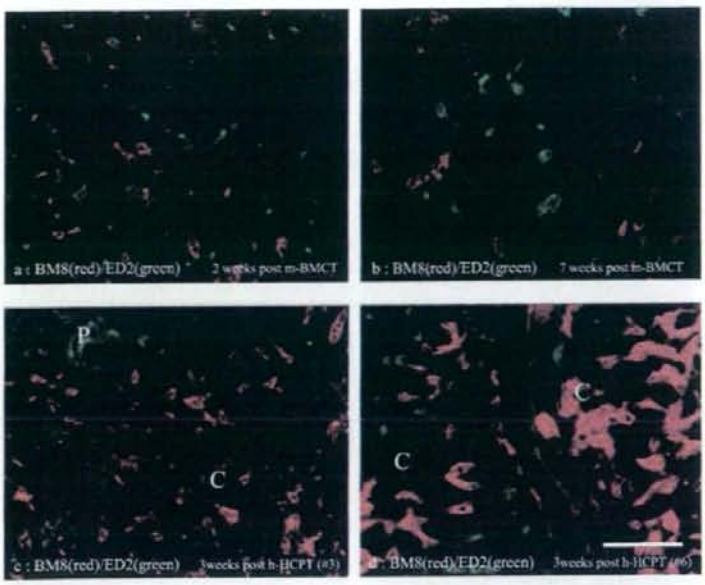

Fig. 5. Distributions of *r*- and *m*-Kupffer cells in the host livers. a and b. Six F344 nude rats were subjected to X-ray irradiation and transplanted with m_{SCID}-BMCs. Rat liver tissues were harvested at 2 weeks (a) and 7 weeks (b) post-*m*-BMCT from three animals each and double-immunostained for the detection of *m*- and *r*-macrophages using the BM8 (red) and ED2 (green) antibodies, respectively. The staining patterns for these antibodies are similar throughout the liver. Similar staining patterns were observed among the animals at each time point. c and d. Liver cryosections from 7 rats (#1–8 except #7) shown in Fig. 2 were prepared at 4 weeks post-*h*-HPCT and stained with the BM8 and ED2 antibodies. Representative photos are shown (c) for rat #5, whose blood *h*-Alb level increased continuously for up to 3 weeks and was > 15 ng/ml at 4 weeks, and (d) for rat #6, whose blood *h*-Alb level was continuously decreased until 3 weeks and was < 10 ng/ml at 4 weeks. The "P" and "C" labels in c and d indicate the portal and central vein regions, respectively. Scale bar = 100 μm.

were used for *h*-hepatocyte transplantation in the present study.

The suppression or deletion of the immunologic reactions of rats for xenotransplantation experiments has been achieved using a number of different methods, including lethal irradiation [6,16,17], an immunosuppressive agent [16], various antibodies [17], and splenectomization [16]. These immunosuppressed rats were utilized in studies of the transplantation of xenogeneic BMCs. Thus, the present study is the first to utilize immunosuppressed rats for the transplantation of xenogeneic tissue parenchymal cells, i.e., *h*-hepatocytes. The replacement rates achieved for xenogeneic BMCs in the previous studies were approximately 40% [17], 60% [6], and 85% [16]. Our conditioning regimen gives a replacement rate as high as 94%, although the number of transplanted *m*-BMCs in the present study is similar to those obtained in the previous studies. Presently, we cannot explain the higher replacement rate, as data on the survival of host BMCs and PBMCs are not available from the previous reports. However, in the present study, the irradiation regimen was more severe and the animals were much younger than that in the previous studies. These two differences may explain the higher replacement rate obtained in our study.

h-Hepatocytes were able to engraft the rat liver in our experimental conditions and proliferated to form small colonies. *h*-Alb was detectable in the blood samples from the hosts. These *h*-hepatocytes expressed several *h*-hepatocyte-specific mRNAs and proteins, which strongly suggests that these cells are able to maintain the original normal phenotypes in disconcordant xenogeneic environments. However, in contrast to SCID mice, the SCID rats did not allow ample proliferation of engrafted *h*-hepatocytes under the conditions that we adopted in the present study. There was no growth of *h*-hepatocyte colonies and no marked increase in blood *h*-Alb concentration, in spite of the high rate of replacement of m_{SCID}-BMCs. Some of the hosts showed small albeit steady increases in blood *h*-Alb levels up to 3 weeks post-*h*-HPCT, although the levels started to decrease at 4 weeks.

Our present data suggest a possible explanation for the low rate of repopulation of *h*-hepatocytes in SCID rats. Recently, it was demonstrated that

interspecies incompatibility of CD47 signaling in macrophages is related to immune responses following xenotransplantation, and the macrophages are activated through the interaction with xenogeneic cells in the liver [10,11]. We classified the chimeric SCID rats into two groups according to the blood level of *h*Alb, rats with *h*Alb > 15 ng/ml and those with *h*Alb < 10 ng/ml at 4 weeks post-*h*-HPCT. The *m*-macrophages were significantly enlarged in the former rats as compared with those in the latter rats. Taken together these facts, we speculate that these activated macrophages play a negative role (s) in the acceptance and proliferation of *h*-hepatocytes, i.e., the transplanted *h*-hepatocytes might be recognized and rejected by activated rat and/or mouse macrophages at 2–4 weeks post-*h*-HPCT. The possibility exists that the high concentration of uPA in the uPA/SCID mice negatively affects the normal functions of Kupffer cells, which permits *h*-hepatocytes to proliferate actively and to repopulate almost completely the host liver. Nevertheless, compared to transplantation into SCID mice, the engraftment rate of *h*-hepatocytes was extremely low in the SCID rats, which suggests a role for uPA in accelerating the engraftment of transplanted *h*-hepatocytes into the liver plate, for example, remodeling hepatic extracellular matrices.

The extent of the hepatic damage seen in the present study is also possibly related to the lower rate of *h*-hepatocyte repopulation. It is known that hepatocytes in the remnant live lobules show higher proliferation activities when the loss of liver volume is higher. We transplanted 2×10^5 *r*-hepatocytes from syngeneic wild-type [dipeptidyl peptidase-IV $(DPPIV)^+$] rats into the retrorsine-treated livers of both 40% PHx and 70% PHx mutant ($DPPIV^-$) rats and compared the repopulation rates of $DPPIV^+$-hepatocytes at 3 weeks post-*r*-HPCT in the 40% PHx and 70% PHx rats. We found that the liver repopulation rate for the 70% PHx rats was 10-fold higher than that for the 40% PHx rats (data not shown).

There are few studies that have transplanted *h*-hepatocytes into the liver of immunotolerant rats [18,19]. The researchers transplanted *h*-hepatocytes into the body cavities or thymus glands of embryonic and newborn rats to induce immunotolerance. Despite the fact that both the hosts and donors were quite young, the rate of hepatocyte engraftment was relatively low [18,19].

In the present study, we demonstrate for the first time that *h*-hepatocytes are capable of engrafting the rat liver and proliferating therein to form colonies. However, the *h*-hepatocytes did not show appreciable replication, as observed for liver-injured SCID mice. Further analyses of the *h*-hepatocyte-bearing SCID rats are necessary to reveal the immunologic mechanisms involved in xenogeneic transplantation, and to generate SCID rats with higher rates of *h*-hepatocyte repopulation.

Acknowledgements

We thank Ms. Y. Yoshizane, Ms. S. Nagai, and Ms. Y. Matsumoto for their excellent technical assistance, and all the members of the Yoshizato group at the Hiroshima Prefectural Institute of Industrial Science and Technology for advice and helpful discussions.

References

1. Lu C, Li AP. Species comparison in P450 induction: effects of dexamethasone, omeprazole, and rifampin on P450 isoforms 1A and 3A in primary cultured hepatocytes from man, Sprague-Dawley rat, minipig, and beagle dog. Chem Biol Interact 2001; 134: 271–281.
2. Guengerich FP. Comparisons of catalytic selectivity of cytochrome P450 subfamily enzymes from different species. Chem Biol Interact 1997; 106: 161–182.
3. Tateno C, Yoshizane Y, Saito N et al. Near completely humanized liver in mice shows human-type metabolic responses to drugs. Am J Pathol 2004; 165: 901–912.
4. Nishimura M, Yoshitsugu H, Yokoi T et al. Evaluation of mRNA expression of human drug-metabolizing enzymes and transporters in chimeric mouse with humanized liver. Xenobiotica 2005; 35: 877–890.
5. Tsuge M, Hiraga N, Takahashi H et al. Infection of human hepatocyte chimeric mouse with genetically engineered hepatitis B virus. Hepatology 2005; 42: 1046–1054.
6. Lubin I, Segall H, Erich P et al. Conversion of normal rats into SCID-like animals by means of bone marrow transplantation from SCID donors allows engraftment of human peripheral blood mononuclear cells. Transplantation 1995; 60: 740–747.
7. Seglen PO. Preparation of isolated rat liver cells. Methods Cell Biol 1976; 13: 29–83.
8. Yamasaki C, Tateno C, Aratani A et al. Growth and differentiation of colony-forming human hepatocytes in vitro. J Hepatol 2006; 44: 749–757.
9. Laconi E, Oren R, Mukhopadhyay DK et al. Long-term, near-total liver replacement by transplantation of isolated hepatocytes in rats treated with retrorsine. Am J Pathol 1998; 153: 319–329.
10. Ide K, Wang H, Tahara H et al. Role for CD47-SIRP-alpha signaling in xenograft rejection by macrophages. Proc Natl Acad Sci USA 2007; 104: 5062–5066.
11. Wang H, Verhalen J, Madariaga ML et al. Attenuation of phagocytosis of xenogeneic cells by manipulating CD47. Blood 2007; 109: 836–842.
12. Mercer DF, Schiller DE, Elliott JF et al. Hepatitis C virus replication in mice with chimeric human livers. Nat Med 2001; 7: 927–933.
13. Meuleman P, Libbrecht L, De Vos R et al. Morphological and biochemical characterization of a human liver in a uPA-SCID mouse chimera. Hepatology 2005; 41: 847–856.

14. Dandri M, Burda MR, Torok E et al. Repopulation of mouse liver with human hepatocytes and in vivo infection with hepatitis B virus. Hepatology 2001; 33: 981–988.
15. Azuma H, Paulk N, Ranade A et al. Robust expansion of human hepatocytes in $Fah^{-/-}/Rag2^{-/-}/Il\text{-}2rg^{-/-}$ mice. Nat Biotechnol 2007; 25: 903–910.
16. Miki T, Lee YH, Tandin A et al. Hamster-to-rat bone marrow xenotransplantation and humoral graft vs. host disease. Xenotransplantation 2001; 8: 213–221.
17. Nikolic B, Cooke DT, Zhao G et al. Both γδT cells and NK cells inhibit the engraftment of xenogeneic rat bone marrow cells and the induction of xenograft Tolerance in mice. J Immunol 2001; 166: 1398–1404.
18. Ouyang EC, Wu CH, Walton C et al. Transplantation of human hepatocytes into tolerized genetically immunocompetent rats. World J Gastroenterol 2001; 7: 324–330.
19. Wu CH, Ouyang EC, Walton C et al. Human hepatocytes transplanted into genetically immunocompetent rats are susceptible to infection by hepatitis B virus in situ. J Viral Hepat 2001; 8: 111–119.

ELSEVIER

Induction of Indoleamine 2,3-Dioxygenase in Livers Following Hepatectomy Prolongs Survival of Allogeneic Hepatocytes After Transplantation

Y.C. Lin, S. Goto, C. Tateno, T. Nakano, Y.F. Cheng, B. Jawan, Y.H. Kao, L.W. Hsu, C.Y. Lai, K. Yoshizato, and C.L. Chen

ABSTRACT

Objectives. Indoleamine 2,3-dioxygenase (IDO), which catalyzes the breakdown of tryptophan into kyneurenine, has immunologic significance for the induction of maternal tolerance and liver allograft tolerance by inhibiting T-cell activation. In the present study, we compared survival of syngeneic or allogeneic hepatocytes in livers with or without hepatectomy. Subsequently, we investigated gene expression and localization of IDO in the recipient liver.

Methods. DA and Fisher 344 rats were used in the following experimental groups: group 1, DA hepatocytes transplanted into hepatectomized Fisher 344 rats; group 2, Fisher 344 hepatocytes transplanted into hepatectomized Fisher 344 rats; group 3, DA hepatocytes transplanted into nonhepatectomized Fisher 344 rats; and group 4, Fisher 344 hepatocytes transplanted into nonhepatectomized Fisher 344 rats. After transplantation, the surviving cells were evaluated on day 5. The IDO signal of the recipient liver was detected by reverse transcriptase polymerase chain reaction (RT-PCR) and immunohistochemistry.

Results. In the hepatectomized groups subjected to allogeneic or syngeneic hepatocyte transplantation, the number of surviving hepatocytes was greater than in the nonhepatectomized group after transplantation. The IDO signals (RT-PCR) in the hepatectomized groups were stronger than those in the nonhepatectomized groups. Immunohistochemistry demonstrated that the IDO signal is located in liver antigen-presenting cells, such as Kupffer cells or dendritic cells, and not expressed in hepatocytes.

Conclusions. Our results demonstrated that IDO is induced in antigen-presenting cells of hepatectomized livers by which subsequently transplanted cells may be protected from rejection by inhibiting indirect or direct recognition of donor antigen and further T-cell activation.

ORTHOTOPIC LIVER TRANSPLANTATION is presently the only therapy that significantly improves the prognosis of liver disease. Unfortunately, the supply of livers available for transplantation is a small fraction of those needed. Transplantation of hepatocytes is a minimally invasive procedure that provides immediate metabolic sup-

From the Department of Surgery and Liver Transplantation Program (Y.C.L., S.G., T.N., Y.F.C., B.J., Y.H.K., L.W.H., C.Y.L.), Chang Gung Memorial Hospital, Kaohsiung Medical Center, Chang Gung University College of Medicine, Kaohsiung Hsien, Taiwan; the Hiroshima Prefecture Institute of Industrial Science and Technology (C.T., C.L.C), and the Department of Biological Science (K.Y.), Hiroshima University, Hiroshima, Japan.

Supported in part by grants from the National Science Council (NSC95-2314-B-182A-152) and Chang Gung Memorial Hospital (CMRPG850071) of Taiwan.

Address reprint requests to Chao-Long Chen, Liver Transplantation Program and Department of Surgery, Chang Gung Memorial Hospital, Kaohsiung Medical Center, Chang Gung University College of Medicine, 123 Ta-Pei Rd, Niao-Sung, Kaohsiung 833, Taiwan, R.O.C. E-mail: clchen@adm.cgmh.org.tw

0041-1345/08/$–see front matter
doi:10.1016/j.transproceed.2008.08.001

port until a donor liver becomes available for transplantation. In contrast to syngeneic hepatocytes, which can survive for long periods and even proliferate in recipients, allogeneic hepatocytes show massive apoptotic cell death due to acute rejection within 1 week after transplantation if not treated with immunosuppression.[1-3]

Indoleamine 2, 3-dioxygenase (IDO) is a cytosolic enzyme catalyzing the oxidative cleavage of the indole ring of l-tryptophan to *N*-formyl-kynurenine. Increasing evidence indicates that IDO suppresses T-cell responses by depleting local tryptophan, an essential amino acid for T-cell proliferation and function, and by the actions of the tryptophan metabolites, such as kyneurenine, which inhibit T-cell viability.[4] In the present study, we compared the survival of syngeneic or allogeneic hepatocytes in livers with or without hepatectomy. Subsequently, we investigated the gene expression and localization of IDO in livers after syngeneic or allogeneic hepatocyte transplantation with or without hepatectomy.

MATERIALS AND METHODS

In this experiment, DA and Fischer 344 rats with dipeptidyl peptidase IV (DPPIV) were used as the hepatocyte source for transplantation. Fischer 344 rats deficient in DPPIV were used as recipients. The experimental design included: group 1, DA hepatocytes (3×10^6) transplanted into 70% hepatectomized Fisher 344 rats (×3); group 2, Fisher 344 hepatocytes (3×10^6) transplanted to 70% hepatectomized Fisher 344 rats (×3); group 3, DA hepatocytes (10^7) transplanted into nonhepatectomized Fisher 344 rats (×3); and group 4, Fisher 344 hepatocytes (10^7) transplanted to nonhepatectomized Fisher 344 rats (×3). After transplantation, the rats were killed at day 5 to evaluate the surviving hepatocytes. Each lobe of the liver was collected in optimal cutting temperature medium or quick-frozen in liquid nitrogen for cryosection and RNA extraction. To calculate the surviving hepatocytes, we performed the DPPIV stain. In reverse transcriptase polymerase chain reaction (RT-PCR) analysis, c-DNA was synthesized by Super-Script-III first strand synthesis kit (Invitrogen, Carlsbad, Calif) and PCR performed using IDO, interferon (IFN)-γ and glyceraldehyde-3-phosphate dehydrogenase (GAPDH) primers. In immunohistochemistry, polyclonal antibodies against rat IDO (Santa Cruz Biotechnology, Santa Cruz, Calif) and monoclonal antibody ED2 to detect macrophages (BMA Biomedicals AG, Switzerland) were used to verify which cells expressed IDO in liver sections.

RESULTS

The surviving hepatocytes were observed in recipient liver sections by DPPIV staining. The numbers of surviving cells in each group were: group 1, 2.9 ± 1.6 cells/mm^2; group 2, 6.1 ± 2.7 cells/mm^2; group 3, 0 cells/mm^2; and group 4, 1.6 ± 1.4 cells/mm^2. RT-PCR analysis revealed that gene expression of both IDO and IFN-γ in the hepatectomized group was stronger than in the nonhepatectomized group (Fig 1). Immunohistochemical analysis demonstrated that IDO signals were located on liver antigen-presenting cells, such as Kupffer cells or dendritic cells, and not expressed in hepatocytes.

DISCUSSION

Recently, some experiments have demonstrated that transplantation of IDO overexpressing cells or organs showed significantly extended survival in recipients.[5,6] Our results also demonstrated that upregulation of IDO in antigen-presenting cells of hepatectomized livers was possibly induced by IFN-γ.[7] As a consequence, the transplanted cells may be protected from rejection by the upregulated IDO, which may directly or indirectly inhibit recognition of donor antigens and subsequent T-cell activation. Overexpression of IDO in the transplanted organ or tissue may act as a local

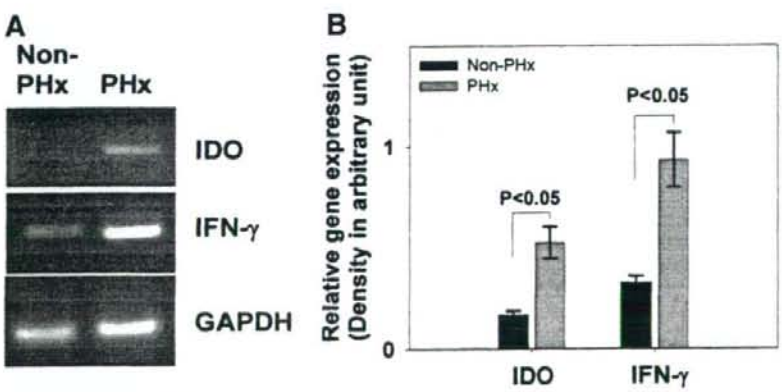

Fig 1. Gene expression of both IDO and IFN-γ are significantly upregulated in the partially hepatectomized (PHx) group compared with those in nonhepatectomized (Non-PHx) group. Rat liver tissues were collected from PHx and non-PHx groups 5 days after allogeneic (DA to Fisher 344) hepatocytes transplantation, followed by RNA extraction and RT-PCR analysis. **(A)** Electrophoresis of both IDO and IFN-γ. **(B)** Densitometric analysis indicates that gene expression of both IDO and IFN-γ in the PHx groups are significantly higher than those in the Non-PHx groups. The statistical analysis is performed using Student's *t*-test; $P < .05$ is considered significant.

immunosuppressive molecule to protect grafts from immune attack.

REFERENCES

1. Song E, Chen J, Min J, et al: FasL expression on splenocytes and its correlation with hepatocytic apoptosis during intrasplenically allogeneic hepatocyte transplantation. Asian J Surg 23:163, 2000

2. Strom SC, Chowdhury JR, Fox IJ: Hepatocyte transplantation for the treatment of human disease. Semin Liver Dis 19:39, 1999

3. Bumgardner GL, Orosz CG: Unusual patterns of alloimmunity evoked by allogeneic liver parenchymal cells. Immunol Rev 174:260, 2000

4. Moffett JR, Namboodiri MA: Tryptophan and the immune response. Immunol Cell Biol 81:247, 2003

5. Alexander AM, Crawford M, Bertera S, et al: Indoleamine 2,3-dioxygenase expression in transplanted NOD islets prolongs graft survival after adoptive transfer of diabetogenic splenocytes. Diabetes 51:356, 2002

6. Liu H, Liu L, Fletcher BS, et al: Novel action of indoleamine 2,3-dioxygenase attenuating acute lung allograft injury. Am J Respir Crit Care Med 173:566, 2006

7. Taylor MW, Feng GS: Relationship between interferon-gamma, indoleamine 2,3-dioxygenase, and tryptophan catabolism. FASEB J 11:2516, 1991

MOLECULAR CARCINOGENESIS 47:784–796 (2008)

Pleiotrophin Inhibits Transforming Growth Factor β1-Induced Apoptosis in Hepatoma Cell Lines

Tae Jun Park,[1] Bo Ra Jeong,[1] Chise Tateno,[2] Hong Seok Kim,[1] Tomohiro Ogawa,[3,4] In Kyoung Lim,[1] and Katsutoshi Yoshizato[2,3,4]*

[1]*Biochemistry and Molecular biology, School of Medicine, Ajou University, Suwon, South Korea*
[2]*Yoshizato Project, Cooperative Link of Unique Science and Technology for Economy Revitalization (CLUSTER), Hiroshima Prefectural Institute of Industrial Science and Technology, Higashihiroshima, Japan*
[3]*Developmental Biology Laboratory, Department of Biological Science, Graduate School of Science, Higashihiroshima, Japan*
[4]*Hiroshima University 21st Century COE Program for Advanced Radiation Casualty Medicine, Hiroshima Liver Project Research Center, Hiroshima University, Hiroshima, Japan*

Pleiotrophin (PTN) is a hepatocyte growth factor and considered to play roles in liver fibrogenesis and hepatocarcinogenesis. In this study we examined the mechanism of the action of PTN in these pathological processes. First, we confirmed that hepatic stellate cells (HSCs) and Kupffer cells, and also later hepatocytes in hyperplastic nodules increased PTN mRNA expressions during carbon tetrachloride-induced liver fibrosis. Then, the relationship between PTN and transforming growth factor β1 (TGFβ1), a known potent pro-fibrogenetic cytokine, in carcinogenesis was investigated using hepatoma cell lines. Huh-7 human hepatoma cells weakly expressed PTN, but HepG2 human hepatoma cells and FaO rat hepatoma cells did not. Recombinant (r) TGFβ1 induced the cultured Huh-7 cells to undergo apoptosis, which was inhibited by rPTN. Huh-7 cells became resistant to TGFβ1-, but not mitomycin C-induced apoptosis when transfected with PTN gene, indicating the specificity of the PTN anti-apoptotic activity. Poly ADP ribose polymerase, procaspase-8 and procaspase-3 were not cleaved in the TGFβ1-reluctant cells. The TGFβ1-induced caspase-3 activation was also suppressed in Huh-7 and FaO cells both transduced with PTN gene-bearing adenoviruses. In summary, PTN was expressed in HSCs, Kupffer cells, and hepatocytes in fibrotic liver. We propose that PTN specifically antagonizes the TGFβ1 activity during liver fibrosis.

Key words: pleiotrophin; TGFβ1; liver fibrosis; hepatocarcinogenesis; caspase-3; hepatic stellate cells

INTRODUCTION

Pleiotrophin (PTN) is a multifunctional cytokine involved in growth, transformation, carcinogenesis, and metastasis [1]. PTN is an 18 kDa heparin binding protein and shows 50% identity to midkine (MK) [2–4]. It promotes the growth of fibroblasts, endothelial cells, and hepatocytes [4–6]. Its gene is grouped as a potent proto-oncogene [7–8]. PTN transforms NIH 3T3 cells in a soft agar plate, and forms highly vascularized tumors [1]. Up-regulation of PTN gene promotes tumor angiogenesis [7]. Furthermore, PTN acts as an angiogenic factor in a paracrine mode for human breast cancer, choriocarcinoma, and melanoma, and seems to be essential for the development of metastasis in melanoma [8].

Previously we identified PTN as a mitogen for rat hepatocytes [9] among proteins secreted by Swiss 3T3 fibroblasts, indicating that PTN plays a role as a hepatocyte growth factor. When co-cultured, rat hepatic stellate cells (HSCs) enhanced the growth of rat hepatocytes by secreting PTN [6]. Furthermore, PTN expression was increased in carbon tetrachloride (CCl_4)-induced fibrotic liver [10]. However, the biological mechanism of PTN in hepatocarcinogenesis has not been clarified yet.

Liver cirrhosis and hepatocellular carcinoma are among the most common liver diseases, and several mechanisms involved in carcinogenesis have been proposed [11–13]. Transforming growth factor β1 (TGFβ1) has been known as a potent fibrogenesis factor [14]. TGFβ1 shows multiple biological properties, including the inhibition of proliferation, the induction of apoptosis, the activation of HSCs, and the promotion of extracellular matrix formation. TGFβ1 expression is low in normal liver, elevated in livers of patients with acute hepatitis, fulminant

Abbreviations: PTN, pleiotrophin; HSC, hepatic stellate cell; CCl_4, carbon tetrachloride; TGFβ1, transforming growth factor β1; PARP, ADP ribose polymerase; PTN-Ad, pleiotrophin adenovirus; LacZ-Ad, LacZ adenovirus.

Chise Tateno's and Katsutoshi Yoshizato's present address is PhoenixBio Co. Ltd., 3-4-1 Kagamiyama, Higashihiroshima, Japan.

*Correspondence to: PhoenixBio. Co. Ltd., 3-4-1 Kagamiyama, Higashihiroshima, Hiroshima 739-0046, Japan.

Received 30 November 2007; Revised 4 February 2008; Accepted 11 February 2008

DOI 10.1002/mc.20438

Published online 31 March 2008 in Wiley InterScience (www.interscience.wiley.com)

hepatic failure, and liver cirrhosis [15]. TGFβ1 is a potent inhibitor of DNA synthesis of cultured hepatocytes and inhibits hepatocyte proliferation after partial hepatectomy [16–18]. The inhibition of TGFβ1 signal effectively prevents fibrosis and preserves the liver function in a fibrotic animal model [19]. These studies all support that TGFβ1 plays pivotal roles in liver fibrogenesis and carcinogenesis.

Apoptosis is essential for normal development and tissue homeostasis. The deregulation of apoptosis and the accelerated proliferate activity of hepatocytes have been reported as significant steps for hepatocarcinogenesis [20,21]. During hepatocarcinogenesis, some of the genetically altered hepatocytes progress to apoptosis and some escape from the apoptosis and undergo carcinogenesis [21]. TGFβ1 is the most effective apoptotic cytokine during hepatocarcinogenesis [22]. TGFβ1 generated the reactive oxygen species and induced apoptosis of Huh-7 cells and activates first caspase-8, -9, and finally -3 [23,24]. Furthermore, a study on "the loss of TGFβ receptor" showed that the hepatocytes in diethylnitrosamine and nodularin-induced-hyperplastic liver nodules escaped from the TGFβ1-induced apoptosis and continued to proliferate [21].

In the present study, we investigated the role of PTN in TGFβ1-induced liver fibrogenesis and carcinogenesis, placing an emphasis TGFβ1-induced apoptosis of hepatocytes. We first demonstrated that HSCs expressed PTN at higher levels. The hepatocytes in hyperplastic nodules formed in a late phase of fibrogenesis started its expression. Then, we focused on the relationship of PTN and TGFβ1 in carcinogenesis using hepatoma cell lines as experimental models. Recombinant (r) PTN suppressed the rTGFβ1-induced apoptosis of cultured hepatoma cells. The mechanism of the anti-apoptotic activity of PTN was studied utilizing hepatoma cells that had been enforced to express PTN gene. The obtained results enabled us to propose that PTN suppresses the apoptosis induced by TGFβ1, but not by mitomycin C, through inhibiting the activation of procaspase-8 and procaspase-3.

MATERIALS AND METHODS

Animal

Nine weeks old Fischer 344 (F344) male rats, weighing 170–180 g, were purchased from Laboratory Animal Center (Shizuoka, Japan), and maintained with standard chow diet and water, ad libitum, under the Institution's guidelines. To induce liver fibrosis, rats were injected subcutaneously with CCl_4 (Wako Pure Chemicals, Osaka, Japan) twice a week for 10 wk at a dose of 2.0 ml/kg body weight. Control rats were injected mineral oil subcutaneously. Five animals were killed at 5, 8, and 10 wk after the CCl_4-administration.

Isolation of Hepatocytes and HSCs

Primary rat hepatocytes were isolated from livers of normal F344 male rats as described previously [25]. Briefly, livers were perfused with collagenase and hepatocytes were harvested by centrifugation at 50*g* for 5 min, and further density gradient centrifugation with 50% Percoll (Amersham, Uppsala, Sweden) at 50*g* for 24 min. The pellet was washed three times with Dulbecco's modified Eagle's medium (DMEM, Gibco BRL, Bethesda, MD), and the cell viability was measured by trypan blue dye exclusion. An HSC-enriched fraction was prepared as reported previously [26]. Briefly, rat livers were digested in situ by perfusion first with 0.07% pronase E (Merck, Darmstadt, Germany) and then with 0.03% collagenase (Wako). They were then excised, broken into small pieces, and digested with 0.08% pronase E, 0.08% collagenase, and 20 μg/ml DNase I (Roche, Mannheim, Germany). The liver cells obtained were suspended in 8.2% Nycodenz (Nycomed, Oslo, Norway) solution and centrifuged with 2,000*g* at 4°C for 20 min. The cells in the upper layer were collected as the HSC-enriched fraction, washed, and suspended in DMEM containing 10% fetal bovine serum (FBS). The mRNA expression level of α-smooth muscle actin (α-SMA) was determined by RT-PCR and used as a measure of the activation of HSCs.

RT-PCR

Total cellular RNAs were isolated from cells of human hepatoma lines (HepG2 and Huh-7), and cells of rat hepatoma cell line (FaO), rat hepatocytes, HSCs, and CCl_4-treated rats liver. First strand cDNA was synthesized using oligo-dT primers from 1 μg of total cellular RNA by reverse transcription reaction in 10 μl reaction volume. The used primers were as follows: human PTN, sense 5′-aaaatgcaggctcaacagtaccagcag-3′ and antisense 5′-cttttaatccagcatcttctcctgttt-3′; rat PTN, sense 5′-aaaatgtcgtcccagcaatatccagcag-3′ and antisense 5′-cttttaatccagcatcttctcctgttt-3′; human glyceraldehyde-3-phosphate dehydrogenase (GAPDH): sense 5′-ggtgctgagtatgtcgtgga-3′ and antisense 5′-gccatgccagtgagcttccc-3′; rat GAPDH, sense 5′-ccatggagaaggctgggg-3′ and antisense 5′-caaagttgtcatggatggatgacc-3′; rat α-SMA: sense 5′-tgtgctggactctggagatc-3′ and antisense 5′-gatcacctgcccatcagg-3′. Amplification were carried out as follows: denaturation at 94°C for 30 s, annealing for 50 s, and extension at 72°C for 50 s. Annealing temperatures were 58°C except 56°C for human PTN. PCR products were separated on 1.5% agarose gels.

Immunohistochemistry

Seven-μm-thick sections were prepared from liver tissues using a cryostat, Leica CM 1900 (Leica Instruments GmbH, Nussloch, Germany), and used for immunohistochemistry with polyclonal antibodies against PTN (N15, Santa Cruz Biotechnology,

Inc., Santa Cruz, CA), α-SMA (Sigma–Aldrich, St. Louis, MO), and ED2, a rat macrophage antigen (Sigma–Aldrich). The sections were treated with 2% normal serum for 20 min, and then incubated overnight with the above antibodies followed by incubation with antibodies with Texas-red and FITC (Zymed, San Francisco, CA) for 60 min. Slides were washed and stained for nucleus with DAPI. The cells were viewed under a fluorescence microscope (Zeiss, Axio Imager M1, Germany).

Induction of Apoptosis by TGFβ1

Cells of human hepatoma cell line, Huh-7, are highly sensitive to TGFβ1 regarding the apoptotic induction [24]. Huh-7 cells were maintained in DMEM containing 10% FBS, and were treated with 1–10 ng/ml of rTGFβ1 (Peprotech EC LTD, London, England) alone or co-treated with 100 ng/ml of rPTN (R&D system, Minneapolis, MN). After 1–3 d of treatment, the cell viability was measured by a MTT assay kit (Promega, Madison, WI): The cells were plated in 96-well microtiter plates at a density of 5×10^3 cells per well and each plate was incubated for 24 h at 37°C in a CO2 (5%) incubator. Each well was washed with phosphate buffered saline (PBS) and incubated with rTGFβ1 in serum-free media for 1–3 d. The cells were counted with the kit according to the instructions provided by the manufacturer, and the absorbance of each well was measured at 450 nm with a microtiter plate reader. Apoptotic changes of nuclear chromatins were observed by staining cells with Hoechst 33342 (Wako): The cells were fixed with paraformaldehyde for 20 min and stained with Hoechst 33342 for 30 min, and 500 cells were counted in randomly chosen areas. The cells with condensed or fragmented nuclei were considered to be apoptotic and their occupancy was expressed as the percentage of apoptosis. TUNEL assay was also employed to confirm the cell death using an Apoptosis Detection Kit (Wako). Apoptosis was induced for normal rat hepatocytes as follows. The cells were maintained in DMEM containing 10% FBS for 1 d and were treated with 2 ng/ml of rTGFβ1 for 2 d. Hoechst staining was performed to detect the apoptosis as above.

Preparation of Hepatoma Cells That Constitutively Express PTN

Huh-7 cells were transfected with pcDNA3 vectors (Invitrogen, San Diego, CA) bearing PTN cDNA with Lipopectamine (Invitrogen), treated with Geneticin (Gibco) for 3 wk at 975 μg/ml concentration for selection. The selected single clones were plated in 24-well culture dishes, treated with trypsin, and collected. As a result, total 4 clones were selected, Huh-7-C2, -C4, -C5, and -C6, and used for further experiments. The expression of PTN in the clones was confirmed by RT-PCR and Western blotting analysis. Similarly, the Huh-7 cells were transfected with pcDNA3 vectors that did not bear the transgene and the obtained cells (Huh-7-V cells) were used as control cells.

Western Blotting for PTN, Poly ADP Ribose Polymerase, Caspase-8, and Caspase-3

rPTN was isolated as below from the media in which Huh-7-C4 and -C5 cells had been cultured for 3 d in the absence of TGFβ1. The collected media were passed through a heparin sepharose column (Biorad, Melville, NY). The absorbed proteins were dissolved in 2×-diluted sodium dodecyl sulfate (SDS) sample buffer consisting of 62.5 mM Tris–HCl (pH 6.8), 2% SDS, with or without 5% β-mercaptoethanol, 10% glycerol, and 0.002% bromophenol blue, and boiled for 5 min. The proteins were separated by 5–15% SDS–polyacrylamide gradient gel electrophoresis, transferred to nitrocellulose membranes (Schleicher & Schuell, Dassel, Germany), and were treated with anti-PTN antibodies (Santa Cruz). Enhanced chemiluminescence (Amersham) reagent was applied to visualize the protein bands. Standard rPTN was purchased from R&D system.

Huh-7-V, -C4, and -C5 cells were cultured for 3 d in the absence and the presence of 5 and 10 ng/ml TGFβ1 and were subjected to Western blotting for poly ADP ribose polymerase (PARP, a substrate of caspase-3 [27]), procaspase-8 and procaspase-3 as follows. Each of the above cells was dissolved in radioimmunoprecipitation (RIPA) buffer consisting of 50 mM Tris, pH 8.0, 150 mM NaCl, 0.1% SDS, 1% NP40, 1 mM phenylmethylsulfonyl fluoride (PMSF), and 1 μg/ml aprotinin. Soluble proteins were loaded on the polyacrylamide gels, and the blots were treated with antibodies against PARP (Zymed), caspase-8 (Santa Cruz), caspase-3 (Cell Signaling Technology, Beverly, MA), and actin (Santa Cruz). Fifty μM of Z-VAD-FMK (Promega) was treated to the Huh-7 cell before 1h of TGFβ1 treatment to inactivate the caspases. The intensity of the actin bands was utilized as a measure for equal loading.

Preparation of Hepatoma Cells Infected With Replication-Defective Recombinant Adenoviruses That Contain PTN Gene

Human PTN cDNA was inserted into replication-defective E1- and E3-adenoviral vectors containing the cytomegalovirus enhancer and the chicken β-actin promoter as a promoter. PTN-expressing adenovirus (PTN-Ad) was amplified in 293 kidney epithelial cells. The cells were disrupted by one cycle of freezing and thawing and centrifuged. PTN-Ad was obtained in the supernatant. Similarly, a vector of bacterial β-galactosidase (LacZ-Ad) was prepared as a control. Huh-7 and FaO cells were plated in 100 mm dishes and infected with 100 m.o.i. of PTN-Ad or LacZ-Ad for 4 h. The cells were trypsinized and plated at a density of 5×10^3 cells per well in 96-well plates.

Two days later, the cells were incubated in the absence or presence of TGFβ1 at 5 ng/ml for up to 2 or 3 d. The expression of PTN and β-galactosidase in the adenovirus-infected cells was confirmed by Western blotting with anti-PTN antibodies on the culture media and galactosidase staining on the infected cells, respectively.

Measurement of Caspase-3 Activity

Huh-7-V cells, Huh-7-C4, and -C5 cells were incubated in the absence or presence of TGFβ1 at 5 ng/ml for up to 3 d. Cell lysates were used for the measurement of the caspase-3 activity using a Caspase-Glo™ Assay kit (Promega) with a luminometer. The net activity of intracellular caspase-3 was calculated by the difference between samples incubated with or without TGFβ1. Similarly, the caspase-3 activity was determined for Huh-7 and FaO cells that had been transfected with PTN-Ad or LacZ-Ad.

Statistical Analysis

Numerical data are presented as the mean ± the standard deviation (SD) of independent determinations. Statistical analysis of differences was performed by Student's *t*-test, with a P value <0.05 being considered significant.

RESULTS

PTN mRNA Expression in Fibrotic Liver, Activated HSCs and Hepatoma Cells

Total RNAs were obtained from hepatoma HepG2, Huh-7, and FaO cells, hepatocytes and HSCs isolated from normal livers, HSCs (activated HSCs) from rats that had been treated with CCl_4 for 5 wk, and livers of rats treated with CCl_4 for 5 wk for measuring PTN mRNA expression levels by RT-PCR. PTN mRNA was undetectable in HepG2 and FaO cells, and in the normal hepatocytes (Figure 1A), but weakly detectable in Huh-7 cells, normal HSCs, and cirrhotic rat liver, and strongly expressed in the activated HSCs. These detected bands were not due to non-specific DNA amplification, because, sequencing of the each gave exactly the same sequence as the expected sequence (data not shown). α-SMA mRNA expression was markedly stimulated in HSCs from the CCl_4-treated rat liver compared to those from the control liver (Figure 1A), which confirmed the activation of HSCs by CCl_4-treatment. From these results we considered possible involvement of PTN in liver fibrogenesis and carcinogenesis.

Distribution of PTN Protein in CCl_4-Induced Fibrotic Liver

Rats were treated with CCl_4 for up to 10 wk and their livers were subjected to immunohistochemical examinations for PTN (Figure 1B). The CCl_4-treatment induced the formation of thick collagen fibers that formed fibrotic septa and the formation of hepatic nodules at 8 wk and thereafter (Figure 1B,c–f). PTN-positive (PTN^+) cells were detectable in nonparenchymal cells of the liver 5 wk post-CCl_4-treatment (Figure 1B,b), but not in the normal liver (Figure 1B,a). The positive cells increased the number as the CCl_4-treatment was prolonged to 8 wk (Figure 1B,c) and 10 wk (Figure 1B,d). The PTN^+-cells were largely in nonparenchymal regions, but some were in hepatic nodules that appeared 8 wk after the treatment (Figure 1B,e). The nodules observed at 10 wk post-treatment also contained the positive cells (Figure 1B,f). These results showed that nonparenchymal cells and hepatocytes in the nodules became PTN^+ during liver fibrosis.

Identification of PTN^+-Cells as Activated HSCs and Kupffer Cells

PTN^+-cells were immunohistochemically characterized. Rats were treated with CCl_4 for 8 wk, and their livers were subjected to double immunohistochemistry for PTN, α-SMA, and PTN, ED2. As shown in Figure 2A, the expression of α-SMA was significantly overlapped with that of PTN, suggesting that activated HSCs might be a major source of PTN-expression in the nonparenchymal cells of liver tissue. Double immunohistochemistry for PTN and ED2 revealed that some of the Kupffer cells also expressed PTN (Figure 2B). These results indicate that both activated HSCs and Kupffer cells express PTN during CCl_4 induced fibrogenesis.

PTN Inhibits TGFβ1-Induced Apoptosis in Huh-7 Hepatoma Cells

The above results strongly suggested the involvement of PTN in liver fibrogenesis. At first, we examined whether PTN shows growth promoting activity on hepatocytes. Huh-7 cells, HepG2 cells, and normal rat hepatocytes were cultured for 1 wk in the presence of rPTN (Figure 3A). PTN increased proliferation of both HepG2 cells and normal rat hepatocytes, but not that of Huh-7 cells. Huh-7 cells, but not HepG2 and normal rat hepatocytes weakly expressed PTN mRNA (Figure 1A), which led us to consider that exogenous PTN was not effective in the proliferation of Huh-7 cells. Next, we examine the role of PTN in hepatic fibrogenesis in relation to the role of TGFβ1, because there have been abundant studies that showed the involvement of TGFβ1 in the pathological process of liver fibrosis [28,29]. We tested the role of PTN in TGFβ1-induced apoptosis in carcinogenesis using Huh-7 cells, because these cells have been known to be sensitive to TGFβ1 in which TGFβ1 induces the apoptosis through activating caspases [24]. Huh-7 cells were co-treated with rPTN (100 ng/ml) and rTGFβ1 (1 and 2 ng/ml) for up to 3 d. The cell number was determined during the culture period (Figure 3B). rTGFβ1 decreased the cell number in a dose-dependent manner. The presence of rPTN in the culture antagonized this action of rTGFβ1. But

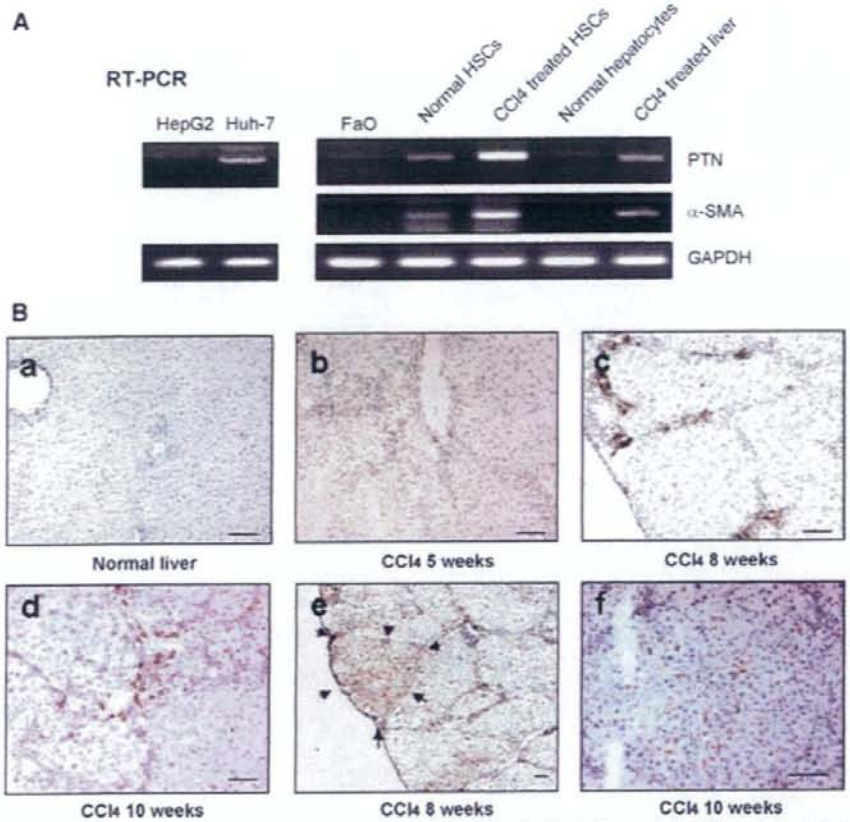

Figure 1. Expression of PTN mRNA and protein. (A) PTN and α-SMA mRNA expression. Total RNA was isolated from HepG2 and Huh-7 cells and subjected to RT-PCR amplification of PTN, α-SMA and GAPDH cDNAs in one series of experiment (left panel) and from FaO cells, HSCs and hepatocytes from normal liver, HSCs from CCl_4-treated liver, and CCl_4-treated liver in another series of experiment (right panel). (B) Distribution of PTN in CCl_4-treated liver. Rats were treated with mineral for 10 d (a), or with CCl_4 for 5 (b), 8 (c and e), and 10 wk (d and f), and their livers were subjected to immunohistochemistry with anti-PTN antibodies. (a) There is no PTN^+-cells. (b) There are a few PTN^+-cells in the nonparenchymal cells. (c) PTN^+-cells are often distributed in the nonparenchymal cells. (d) Distribution of PTN^+-cells is similar as in c. (e) A nodule is positive for PTN. (f) A nodule is positive for PTN. Arrows in e indicate the PTN^+-liver nodule. Bar represents 100 μm.

when treated with more than 5 ng/ml of TGFβ1, the cells were unable to escape from the apoptosis even in the presence of PTN (data not shown). The cells were stained with Hoechst 33342 and examined for the presence of chromosomal condensations (Figure 3C). TGFβ1 evidently induced the apoptotic changes of chromatin. The frequency of cells with such changes was counted on the photographs (Figure 3D). rTGFβ1 at 2 ng/ml increased the apoptosis rate >3-fold compared to that of the control cells. The presence of rPTN at 100 ng/ml significantly decreased the rTGFβ1-stimulated level to <50%. These results support the previous report that TGFβ1 enhances the apoptosis of Huh-7 cells [24]. Identical experiments were undertaken using normal rat hepatocytes (Figure 3E and F). Although the induction rate was less than in Huh-7 cells, TGFβ1 at 2 ng/ml also induced the apoptotic change in chromatin, which was significantly inhibited by PTN.

Establishment of PTN Gene-Expressing Huh-7 Cells

To further investigate the anti-"TGFβ1-induced apoptotic function" of PTN, we established a PTN gene-expressing Huh-7 cell line. RT-PCR showed that Huh-7 cells themselves weakly expressed PTN mRNA, but its proteins were undetectable by Western blotting (Figure 4A). We transfected pcDNA3-PTN to Huh-7 cells and selected out the single cell colonies designated Huh-7-C2, -C4, -C5, and -C6 as